

# EXPLORING GRAVITATIONALLY-LENSED $Z \gtrsim 6$ X-RAY AGN BEHIND THE RELICS CLUSTERS

ÁKOS BOGDÁN<sup>1</sup>, ORSOLYA E. KOVÁCS<sup>2,1</sup>, CHRISTINE JONES<sup>1</sup>,  
WILLIAM R. FORMAN<sup>1</sup>, RALPH P. KRAFT<sup>1</sup>, VICTORIA STRAIT<sup>3</sup>, DAN COE<sup>4</sup>, AND MARUŠA BRADAČ<sup>3</sup>

<sup>1</sup>Harvard Smithsonian Center for Astrophysics, MA, USA, <sup>2</sup>Masaryk University, Brno, Czech Republic,

<sup>3</sup>Department of Physics, University of California, CA, USA

<sup>4</sup>Space Telescope Science Institute, MD, USA

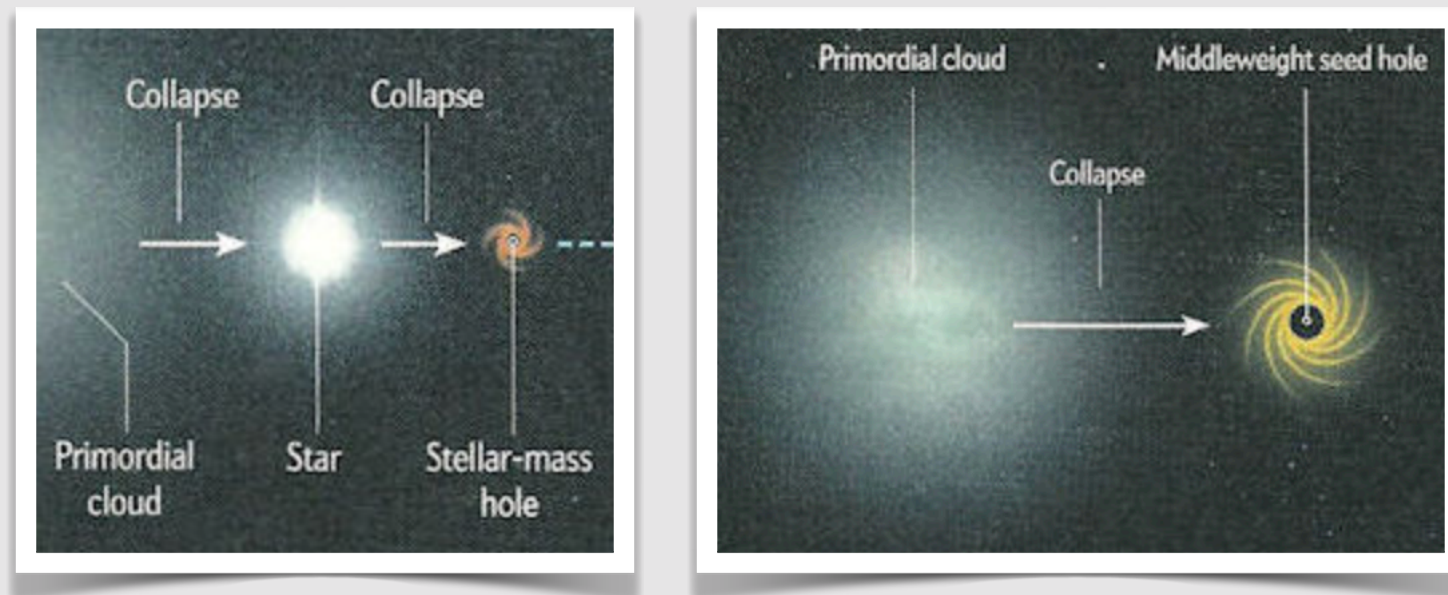
*ApJ*, 2022



Abell 2163, credit: ESA/Hubble & NASA

# BH formation scenarios

- **deep optical surveys:** >200 bright quasars at  $z > 6 \rightarrow$ 
  - accretion-powered black holes in the center of galaxies (BHs) already exist  $\sim 1$  billion years after the Big Bang
  - $10^9 M_{\odot}$  (this is the high-end tail of BH mass distribution)
  - rapid assembly



- various seeding models explain the origin of BHs
  - **"light seed" scenario** (low-mass BH seeds)
    - collapse of Population III stars  $\rightarrow$  BH seeds with  $10 - 100 M_{\odot}$
    - rapid growth via accretion /mergers within 1 billion years
  - **"heavy seed" scenario** (massive BH seeds)
    - direct collapse of massive gas clouds  $\rightarrow$  BH seeds with  $10^4 - 10^5 M_{\odot}$  BH
    - episodic accretion

- **aim of this study: constraining the formation scenarios of BHs**

# Constraining formation scenarios

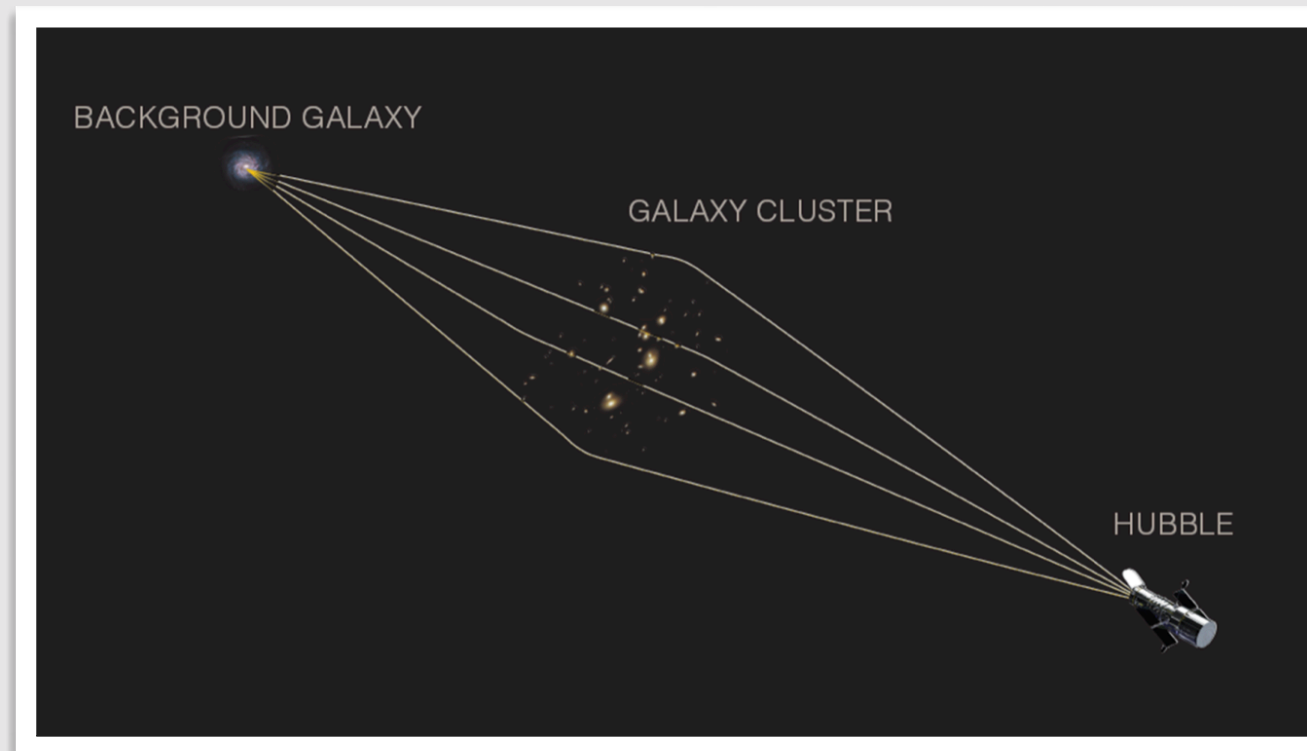
- main (X-ray) observational differences: **luminosity (this work)**, accretion density, number of BH seeds (occupation fraction)
- observations of BHs at the "cosmic dawn" is demanding for present-generation X-ray observatories due to the
  - low luminosity of BHs
  - low sensitivity of telescopes

## Previous X-ray studies

- **X-ray follow-up observations** of optically-identified quasars with Chandra
  - $z \sim 6$  AGN from the high-end tail ( $\sim 10^9 M_{\odot}$ ) of BH mass distribution
  - these AGN are not representative
- **Chandra Deep Field South**
  - average properties of medium-redshift ( $z = 2 - 5$ ) AGN
  - most notable: Vito et al. 2016, stacking  $\rightarrow z \approx 4 - 5$  AGN detection, but no  $z \approx 6$  (only upper limit)
- **Gravitational lensing in X-ray**
  - Cluster Lensing And Supernova survey with Hubble (CLASH) clusters
  - individual AGN detections at  $z = 2.8 - 5$ , but not at  $z \approx 6$

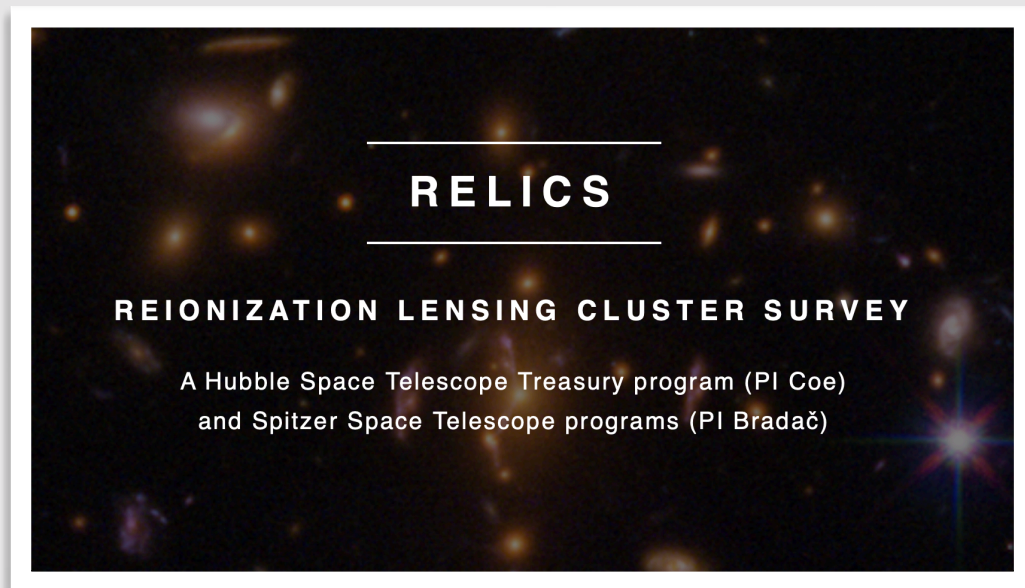


## This study



- **gravitational lensing on X-ray data** to magnify fainter AGN
- lensing objects: galaxy clusters
  - magnification of background galaxies
  - no magnifying effect on foreground objects (cluster emission, sky & instrumental background)
- 1<sup>st</sup> approach: search for individual AGN in background galaxies with amplified signal
- 2<sup>nd</sup> approach: stacking the amplified signal to further boost signal-to-noise ratios & to probe average characteristics of BHs
- data used in this study:
  - Chandra images
  - HST & Spitzer catalog of lensed galaxies identified in the RELICS survey (from Salmon et al. 2020)

# RELICS clusters & background galaxies

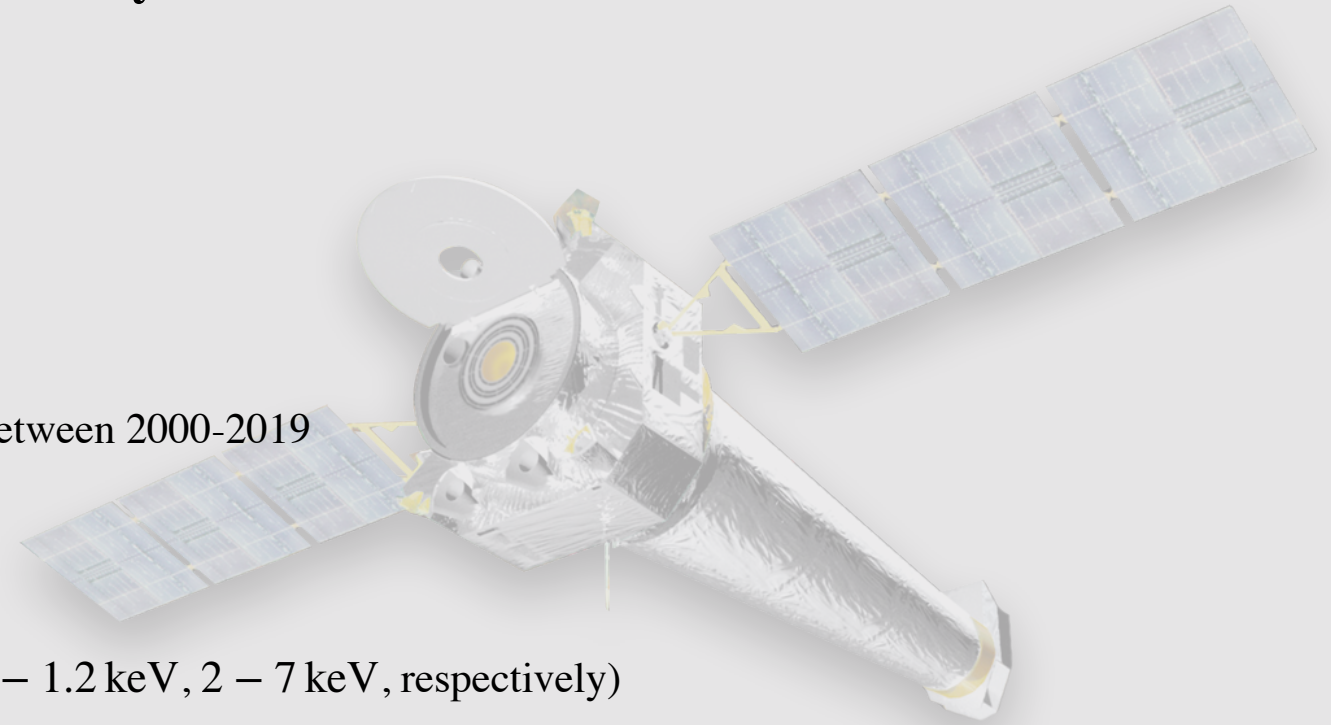


- imaging of strongly lensed fields i.e. of 41 galaxy clusters
- cluster redshifts:  $z = 0.18 - 0.97$
- science topics: high-redshift galaxies, AGN etc.

- high-resolution Chandra observations of 35 RELICS clusters
- El Gordo (ACT-CLJ0102-49151) cluster excluded from our cluster sample due to its extremely bright ICM
- galaxy sample consists of lensed galaxies behind the remaining 34 galaxy clusters
  - 174 HST&Spitzer-identified galaxies with redshifts of  $6 < z < 8$  behind the 34 clusters (Strait et al. 2021)
  - SED fitting of HST & Spitzer fluxes  $\rightarrow$  physical characteristics of the galaxies (photometric redshift, stellar mass, star formation rate etc.) (Strait et al. 2021)
  - based on photometric redshift, 19 low-redshift galaxies were excluded from the sample
  - **final galaxy sample:** 155  $z \approx 6$  galaxies
  - lensing magnification ( $\mu$ ) at the location of the galaxies from cluster lensing magnification maps from Strait et al. 2021
    - $\mu = 1 - 95$

## Chandra analysis

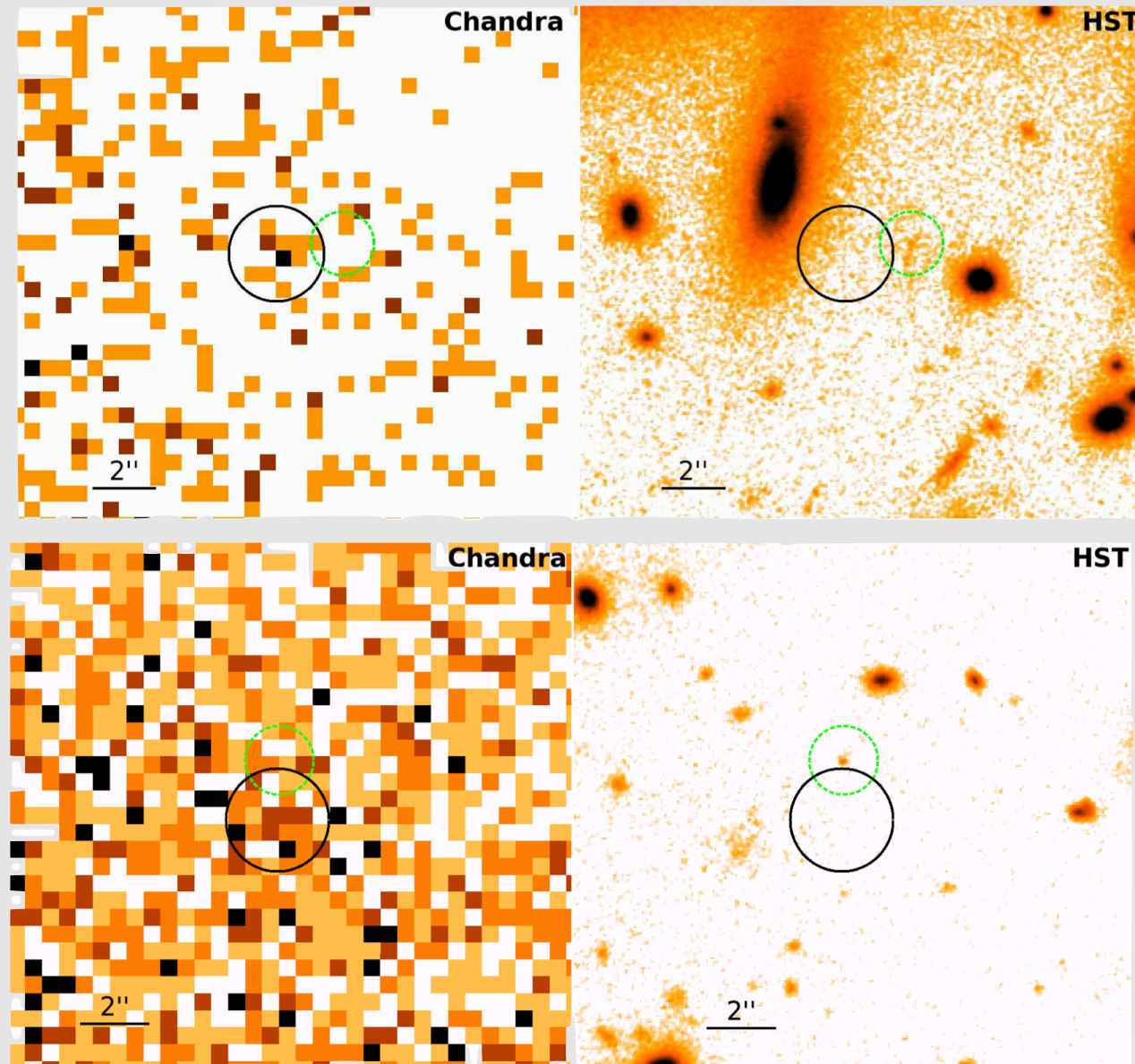
- data were obtained from public archive
- 105 high-resolution ACIS-I & ACIS-S imaging observations taken between 2000-2019
- total exposure time is 3.53 Ms
- analysis with standard CIAO tools
- image extraction in the broad, soft, and hard band (0.5 – 7 keV, 0.5 – 1.2 keV, 2 – 7 keV, respectively)
- images and exposure maps of clusters observed in multiple pointings were merged



## Results, individual detections

1. source detection with CIAO wavdetect (this detects mainly low-redshift AGN)
  2. cross-correlation of the X-ray source list with the HST galaxy positions
    - differences in astrometric accuracy between Chandra and HST (Liu et al. 2021, largest offset  $< 0.8''$ )
    - broader Chandra point spread function at the edges of the detector
    - search radius:  $2.5''$
- **results:** two X-ray point sources in the proximity of lensed galaxies:
  - match #1 in cluster MACS0553-33
    - offset:  $2.1''$
    - $L_X$  assuming the distance of the galaxy ( $z = 6.55$ ):  $4.6 \times 10^{43} \text{ erg s}^{-1}$
  - match #2 in cluster PLCKG237+32
    - offset:  $1.7''$
    - $L_X$  assuming the distance of the galaxy ( $z = 7.82$ ):  $3.5 \times 10^{44} \text{ erg s}^{-1}$
  - chance coincidence?
  - Monte Carlo simulations  $\rightarrow$  we expect  $\approx 0.23$  random matches in our sample  $\rightarrow$  one or even two X-ray sources are associated with a high-redshift galaxy
  - **major caveat:** relatively large projected offsets (11.7 kpc & 8.5 kpc at the redshift of corresponding galaxy)  $>$  half-light radius of typical galaxies at  $z \sim 6$

## Results, individual detections



The potential matches between the X-ray sources and high-redshift AGN for MACS0553-33 (top panel) and PLCKG287+32 (bottom panel). The left panels show the 0.5 – 7 keV band Chandra images and the right panels show the multi-color HST images of the regions around the sources. The images are centered on the X-ray sources (black solid circle) that are in the vicinity of galaxies at  $z = 6.55$  and  $z = 7.82$  (dashed green circles). The projected distances between the centroids of the X-ray point sources and the high-redshift galaxies are 2.1'' and 1.7'' for the source in MACS0553-33 and PLCKG287+32, respectively. However, due to the relatively large projected distance, the X-ray sources are unlikely to be associated with the high-redshift galaxies.

# Results, stacking the high-redshift galaxies

- analysis steps:

1. source exclusion
2. cutout images and exposure maps around each galaxy
3. stacking the cutout images and exposure maps → increased signal-to-noise ratios & detection likelihood
4. magnification correction on net count rates

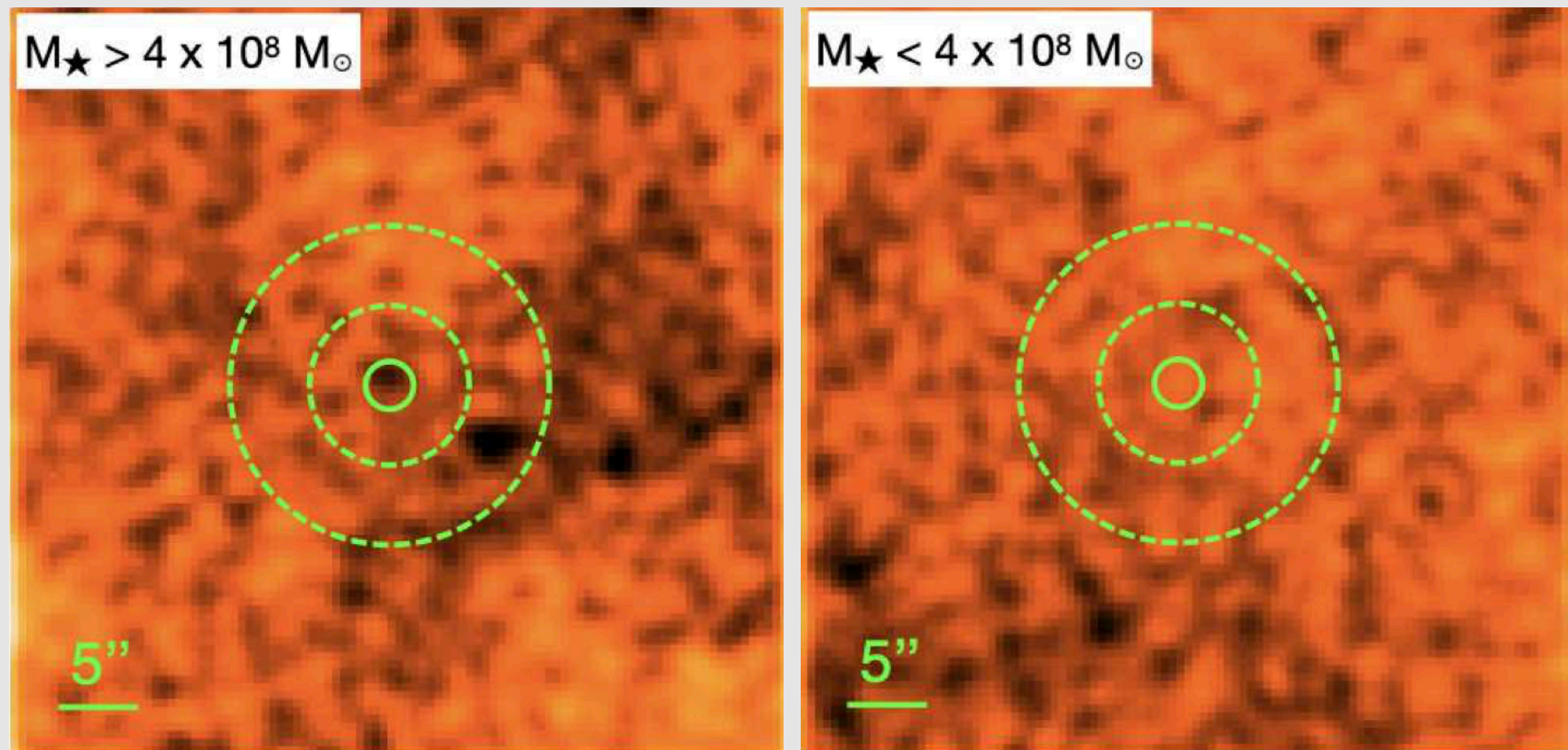
- multiple approaches of stacking:

1. stacking **all** 155 galaxies together
2. stacking the subsample of low- ( $< 4 M_{\odot} \text{ yr}^{-1}$ ) and high-**SFR** ( $> 4 M_{\odot} \text{ yr}^{-1}$ ) galaxies separately
3. low- ( $\log \mu < 0.5$ ) and high-**lensing-magnification** ( $\log \mu > 0.5$ ) galaxies
4. low- ( $M_{\star} < 4 \times 10^8 M_{\odot}$ ) and high-**stellar-mass** ( $M_{\star} > 4 \times 10^8 M_{\odot}$ ) galaxies

- **result:** weak ( $2.2\sigma$ ) detection only in the high-mass sample

- Jackknife resampling confirms the detection → only  $\sim 0.3\%$  of the random resampling simulations show  $\geq 2.2\sigma$  detections.

## Results, stacking the high-redshift galaxies



Stacked 0.5 – 7 keV band Chandra images of lensed high-redshift galaxies using stellar mass as binning criteria. We obtained a weak,  $2.2\sigma$  detection for the high-mass sub-sample, while other sub-samples remained undetected.

# Constraining the properties of $z \sim 6$ BHs

- constraints from the stack of all 155 galaxies:
- estimating the BH mass using two approaches:
  1. luminosity upper limit  $L_{0.5-7\text{keV}} \lesssim 8.4 \times 10^{41} \text{ergs}^{-1}$   $\rightarrow$  in case of accretion at Eddington rate the mean BH mass of the sample is  $< 6.7 \times 10^4 M_{\odot}$
  2. mean stellar mass of the galaxy sample is  $1.3 \times 10^9 M_{\odot}$   $\rightarrow$  BH mass–stellar bulge mass scaling relation (Schutte et al. 2019)  $\rightarrow$   $2.6 \times 10^6 M_{\odot}$  for the mean BH mass  $\rightarrow$  40 times larger
- possible explanations:
  - the scaling relation only valid locally, and high-redshift BHs are much less massive
    - this explanation is incompatible with some observational studies, e.g.
      - Merloni et al 2010: high-redshift BHs may be over-massive relative to their host galaxies
      - Bogdán et al. 2012: some high-redshift BHs may grow faster than their host galaxies
  - BHs accrete at a few per cent of their Eddington rate  $\rightarrow$ 
    - **low mean accretion rate supports the "heavy seed" scenario:** BHs may experience episodic periods with high accretion rates, while most times they accrete at low Eddington rates

# Summary

- Chandra analysis of 155 high-redshift ( $z \approx 6$ ) gravitationally-lensed galaxies identified by Hubble behind 34 RELICS clusters
- probing the X-ray emission both individually and in stacks
- search for individual high-redshift AGN revealed two X-ray source–high-redshift galaxy pairs, but due to their large offset, X-ray sources are not likely associated with a high-redshift galaxy
- stack of 155 high-redshift galaxies resulted in non-detection  $\rightarrow$  upper limit on luminosity and BH mass
- the upper limit on the luminosity implies that typical high-redshift BHs accrete at a few per cent of their Eddington rate
- splitting the sample based on stellar mass, SFR, and lensing magnification
- stack of massive galaxies resulted in a  $2.2 \sigma$  detection, other subsamples remained undetected

## Future studies

- high-redshift galaxies behind Hubble Frontier Field clusters
- high-redshift galaxies behind Abell 2744, which is a JWST target in its early release science program + **2.1 Ms Chandra VLP project** (PI: Ákos Bogdán, me: Co-I)



A2744, credit: Chandra / HST